

MFM observation of spin structures in nano magnetic dot arrays fabricated by damascene technique

K. Sato^a, T. Yamamoto^a, T. Tezuka^a, T. Ishibashi^a, Y. Morishita^a, A. Koukitu^a,
K. Machida^{a,b}, T. Yamaoka^c

^aTokyo University of Agriculture and Technology, Koganei, Tokyo 184-8588, Japan

^bScience and Technology Research Laboratory of NHK, Setagaya-ku, Tokyo 157-8510, Japan

^cSII Nanotechnology Ltd., Matsudo, Chiba 270-2222, Japan

Elsevier use only: Received date here; revised date here; accepted date here

Abstract

Regularly aligned array of magnetic nano dots buried in silicon wafers have been fabricated using damascene technique with a help of electron beam lithography. Arrays of square, rectangular, cross-shaped and Y-shaped structures of submicron size have been obtained. Spin distributions have been observed by means of magnetic force microscopy (MFM) and analyzed by a micromagnetic simulation with Landau-Lifshitz-Gilbert (LLG) equations. Importance of magnetostatic interactions working between adjacent dots has been elucidated.

© 2005 Elsevier B.V. All rights reserved

68.37.Rt; 75.60.Ch; 75.75.+a

Keywords: nano magnetic dots; magnetic force microscopy; Landau-Lifshitz-Gilbert equation; magnetostatic interaction

1. Introduction

Studies of spin distributions in nano or submicron scale magnetic dots with different pattern shapes are attracting interest since the state-of-the-art technology for high density magnetic storages is based on magnetic structures as small as a few tens of nanometer in size. We have been working with fabrication of arrays of submicron permalloy (Fe₂₀Ni₈₀) patterns buried in a silicon wafer using a damascene technique.¹

Arrays of square, rectangular, cross-shaped and Y-shaped structures of submicron size have been obtained. Isolated square dot of 1 μm in size shows a closure-domain image consisting of four domains separated by 90°-domain walls. In a system where the distance between adjacent dots is as close as a few hundred nanometers, spin-structures become strongly influenced by a magnetostatic interaction. We experimentally observed that the chirality of the spin flow in the closure domain pattern is reversed between two adjacent dots, the result having been explained in terms of the magnetostatic interaction by solving the Landau-Lifshitz-Gilbert equation.²

In the cross-shaped pattern were observed the magnetic poles as two pairs of bright and dark spots at the ends of the cross-bars, as well as the complicated spin structure at the crossing region. The force gradient distributions were simulated based on micromagnetic calculations taking into account the stray field from the MFM tip using the integral equation method.³

We recently prepared two different arrangements of Y-shaped patterns of submicron size. The spin distribution in the three-arm structure is of current interest since in such a system the geometric frustration effect plays an important role.⁴

In this paper we briefly review our previous results and describe our recent results on the Y-shaped patterns.

2. Experiments

The specimens used in this study were prepared by the damascene technique as described in the following: We employed a Si(100) wafer as a substrate to fabricate magnetic structures. An EB-resist (ZEP-520 supplied by Nippon Zeon Co. Ltd.) which has an excellent dry-etching resistance was spin-coated at a rotation speed of 5000 rpm for 90 s, followed by baking at 160°C for 20 min before EB exposure. The thickness of the resist was about 35 nm. Arrays of square, rectangular dots as well as cross-shaped and Y-shaped dots as shown in Fig. 1 were patterned on the resist using an electron beam pattern generator (JEOL type JBX-5000SH in TUAT or ELIONIX type ELS-7300ULH in NHK). The patterned resist was developed using a ZED-N50 (n-Amyl acetate) developer for 2 min. The patterned area was as large as 3 mm × 3 mm.

Using the patterned resist as a mask, the Si substrate was processed by a plasma-etching using CF₄ gas with an RF power of 400 W. The optimum etching rate was found to be about 0.1 μm per minute. The remained resist was finally removed in an ultrasonic bath using acetone.

By this method, arrays of pits of approximately 150 nm in depth were uniformly formed over the patterned area on the Si wafer. Permalloy films were deposited using an electron beam (EB) evaporator. Thickness was monitored during evaporation by a quartz thickness monitor to adjust the evaporation period to adjust the thickness equal to the pit depth.

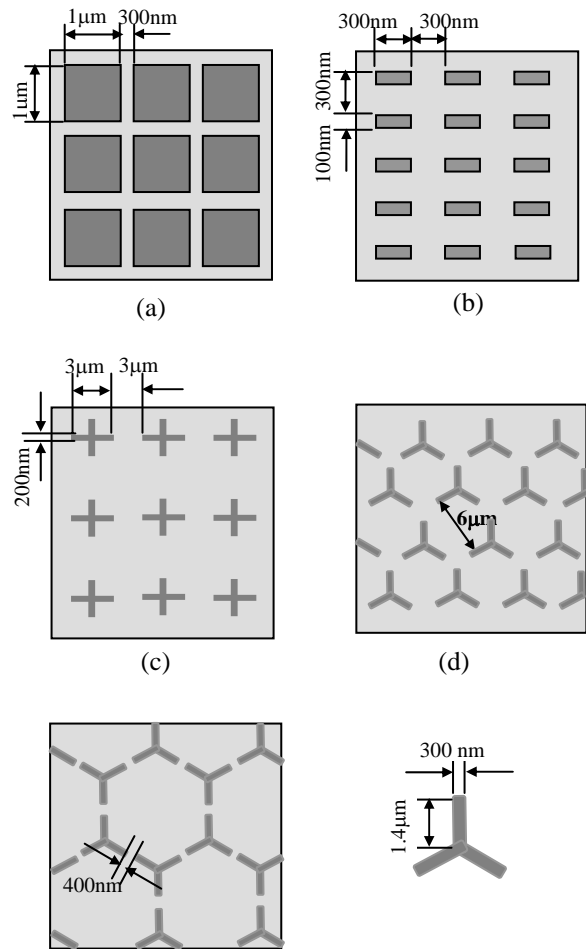


Fig. 1 Designed mask patterns of (a) square, (b) rectangular, (c) cross, (d) Y-shaped (linear well-spaced alignment) and (e) Y-shaped (honeycomb alignment) dot arrays.

Typical deposition rate was 1.0 Å/s.

The magnetic film outside the pit was polished out to obtain a flat surface by means of the chemical mechanical polishing (CMP) using a pH-controlled chemical solution including a polishing slurry (Glanzox SP-15, Fujimi Corp.). The polishing rate was optimized by adjusting combination of a mechanical polishing and an etching for chemical reaction. The typical rms roughness after the CMP process was less than 10 nm.

Microscopic spin structures were observed using an SII Nanotechnology type SPI-4000/SPA300HV

MFM with a low-moment tip (coated with 25 nm-thick CoCrPt) using a specially designed Q-control in the high vacuum environment. The measurements using the low-moment tips were carried out at SII-Nanotechnology Inc.

3. Micromagnetic simulations

Micromagnetic simulations using the Landau–Lifshitz–Gilbert equation were carried out to explain the observed MFM images of the cross-shaped nano-scale patterns. The micromagnetic simulator⁵ was modified to correspond to a complicated three-dimensional (3D) pattern, which was created using a generic 3D-CAD system. The equation was numerically solved using the fourth order Runge–Kutta method for high accuracy.

To demonstrate the MFM images, the interaction between the magnetization of the tip and the stray field of the sample was evaluated. The MFM output signals are proportional to the force gradient between the tip and the sample. The force gradient is given by

$$\frac{\partial F_z}{\partial z_{tip}} = \int_{sample} \frac{\partial^2 \mathbf{H}_{tip}}{\partial z^2} \cdot \mathbf{M}_{sample} d^3r + \int_{sample} \frac{\partial \mathbf{H}_{tip}}{\partial z} \cdot \frac{\delta \mathbf{M}_{sample}}{\delta z_{tip}}$$

where \mathbf{H}_{tip} is the stray field from the tip at the sample volume element, \mathbf{M}_{sample} is the magnetization of a sample volume element at equilibrium, and z_{tip} is the tip–sample distance.⁶ The values of \mathbf{H}_{tip} and \mathbf{M}_{sample} are considered to change corresponding to the tip–sample interaction.

4. Results and discussion

The MFM image of the square pattern (1 $\mu\text{m} \times 1 \mu\text{m}$) shown in Fig. 2(a) clearly demonstrates a closure domain structure with 90°-domain walls. The

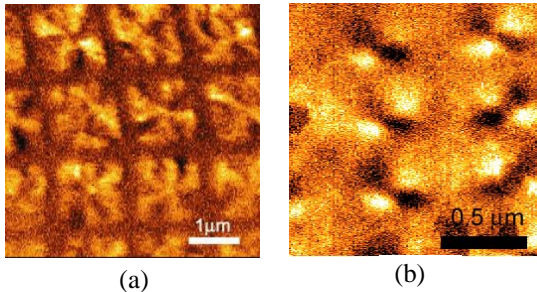


Fig. 2 MFM images of (a) square and (b) rectangular shaped dot arrays

propeller-like distortion of the domain wall pattern, which was ascribed to the stray field from the tip by Miltat, is clearly observed even with a low-moment tip. This means the propeller-like distortion is not necessarily due to the stray field of the MFM tip. In addition, a careful observation suggests that the direction of rotation (chirality) in the propeller-shaped domain walls of adjacent square dots shows a mirror-reflection of each other, suggesting a strong effect of magnetostatic interactions between dots in the array structure.

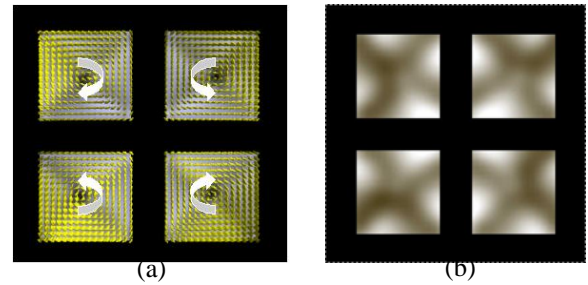


Fig. 3 (a) Simulated spin structures by the micromagnetic calculation using LLG equation (b) force-gradient image calculated taking into account the tip–sample interaction.

Simulation was carried out in the model structure consisting of four square dots with a dimension of 200 nm \times 200 nm \times 20 nm with 50 nm separation between dots. The calculated spin structure is illustrated in Fig. 3(a), in which a closure domain structure with the 90°-wall appears. The chirality of the spin direction in adjacent dots is opposite to each other as shown by white arrows. Figure 3(b) is the Z-component force-gradient image taking into account the tip–sample interaction, providing a good agreement with the MFM patterns shown in Fig. 2(a).

On the other hand the MFM image of the rectangular dot (100 nm \times 300 nm) shows a checker pattern as shown in Fig. 2(b), in contrast with the case of circular dots of 100 nm in diameter, for which we confirmed single domain spin structure. The spin structure as observed in Fig. 2(b) was similar to that described in the literature.⁷ The black and white contrast seems randomly aligned between adjacent dots, suggesting that the magnetostatic interaction has no strong influence in the present case.

Figure 4 shows the MFM images of the cross-shaped dot array, in which figure (a) shows a wide-area-scan image and (b) a narrow-area-scan image

around the crossing region. Regularly aligned magnetic poles are observed in the MFM image shown in Fig. 4(a). Dark spots appear on the left and lower ends of the crossed bars, whereas bright spots on the right and upper ends. At the crossing point of cross-bars are observed a complicated MFM image at the crossing region as illustrated in Fig. 4(b).

The results of the LLG simulation are illustrated in Fig. 5. Figure 5(a) shows a force-gradient image, and is found to show a remarkable agreement with the experimental MFM image of Fig. 4(a): Both theoretical and experimental images show dark or bright images of magnetic poles at the end of the cross-bars. From a three dimensional illustration of the spin structure at the end portion of the bar, an inclination of spins with vortex structure exists only at the end portion of the bar. The formation of the vortex may be consequence of fact that the height (150 nm) of the buried magnetic pattern is comparable to the width (200 nm) of the cross-bar.

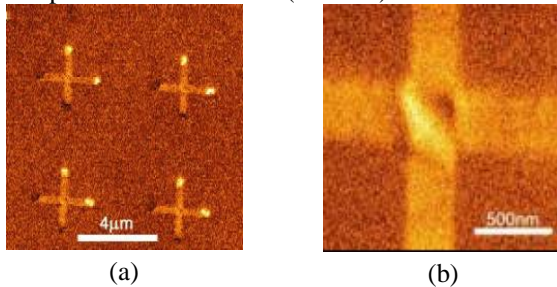


Fig. 4 MFM observation of cross-shaped dot array (a) included 4 dots (b) zoom up around the crossing region

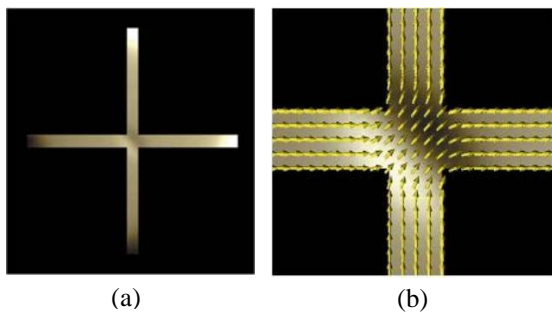


Fig. 5 Result of LLG simulation. (a) Force-gradient image taking into account tip-sample interaction, (b) spin flow image at the crossing region

As shown in Fig. 5(b) the spin flows continuously from the lower left to the upper right in the figure at the crossing region with a vertical inclination along the diagonal line. Thus the complicated spin structures observed in Fig. 4(b) at the crossing point have been explained by the simulation. Evaluation of magnetostatic interactions between crosses is the issue for future investigations.

A SEM micrograph of the linearly aligned array of Y-shaped magnetic dots with spacing as long as 6 μm is shown in Fig. 6.

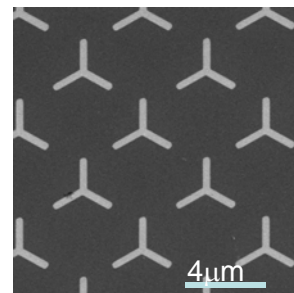


Fig. 6 SEM micrograph of the linearly aligned array of Y-shaped pattern (design: Fig. 1(d)) after CMP process

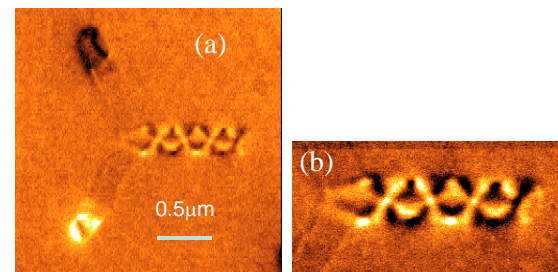


Fig. 7 MFM image of (a) the Y-shaped dot and (b) the magnified pattern in the arm without poles

An MFM image in the Y-shaped dot is illustrated in Fig. 7(a). Magnetic poles are observed at the end of the single domain images in two of the three arms of the Y-shapes pattern. On the other hand, a multi-domain structure is observed on the remaining arm, for which the magnified MFM image is given in Fig. 7(b). A preliminary result of the LLG simulation reproduces a multi-domain spin structure in one of the three arms of the Y-pattern.

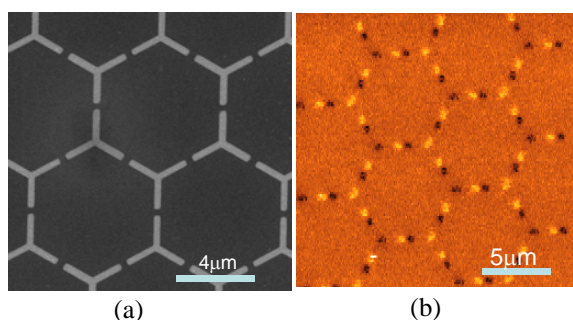


Fig. 8 SEM micrograph of the honeycomb arrangement of Y-shaped patterns

Closely-spaced honeycomb arrangement of Y-shape pattern is successfully fabricated as shown in the SEM micrograph of Fig. 8(a). An MFM image is illustrated in Fig. 8(b), in which regularly arranged black and white spots are observed. The direction of magnetization in each arm is found to be determined to satisfy the “two-in, one-out” or the “one-in, two-out” rule around the vertex, similar to the case described in ref. 4.

Magneto-optical image of the same specimen has recently been obtained using a specially-designed high sensitivity magneto-optical Kerr microscope.⁸ The pattern is much different from the MFM image shown in Fig. 8(b). Difference may be caused by the fact that magneto-optical Kerr effect does not detect a magnetic flux as does the MFM, but detects only a vertical component of the sample magnetization. Detailed analysis is underway and will be published in our later publications.

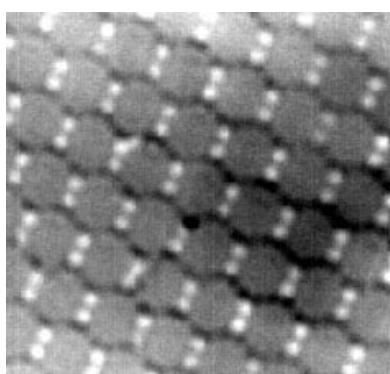


Fig.9 Magneto-optical image of the honeycomb arrangement of Y-shaped patterns

5. Conclusion

Regularly aligned magnetic patterns with different shapes have been fabricated by a damascene technique. MFM observation revealed a closure domain for the square dot array, a checker pattern for the rectangular dot array, and magnetic poles for cross-shaped pattern. For separated Y-shaped pattern magnetic poles appear on two of the three arms and multi domain on the rest. For honeycomb arrangement regularly-aligned magnetic poles are observed. Importance of magnetostatic interaction is elucidated.

Acknowledgments

This work has been carried out under the 21 st-century COE program of TUAT on “Future Nano Materials”.

References

- ¹ T. Matsumoto, T. Tezuka, T. Ishibashi, Y. Morishita, A. Koukitu and K. Sato, *Trans. Magn. Soc. Jpn.* **3** (2003) 103
- ² T. Tezuka, T. Yamamoto, K. Machida, S. Shimizu, T. Ishibashi, Y. Morishita, A. Koukitu and K. Sato, *Trans. Magn. Soc. Jpn.* **4** (2004) 241.
- ³ K. Machida, T. Tezuka, T. Yamamoto, T. Ishibashi, Y. Morishita, A. Koukitu, K. Sato, *J. Magn. Magn. Mater.* **290-291** (2005) 779.
- ⁴ E. Saitoh, M. Tanaka and H. Miyajima, *J. Appl. Phys.* **93** (2003) 7444.
- ⁵ K. Machida, N. Hayashi, Y. Yoneda, J. Numazawa, M. Kohro, T. Tanabe, *J. Magn. Magn. Mater.* **226-230** (2001) 2054.
- ⁶ J.M. Garcia, A. Thiaville, J. Miltat, K.J. Kirk, J.N. Chapman, F. Alouges, *Appl. Phys. Lett.* **79** (2001) 656.
- ⁷ A. Hubert, R. Schäfer, *Magnetic Domains—The Analysis of Magnetic Microstructures*, Springer, New York, 1998.
- ⁸ T. Ishibashi, Z. Kuang, Y. Konishi, K. Akahane, X. R. Zhao, T. Hasegawa and K. Sato, *Trans. Magn. Soc. Jpn.* **4** (2004) 278.